

Efficient Private Inference Based on Helper-Assisted Malicious Security Dishonest Majority MPC

Kaiwen Wang, Yuehan Dong, Junchao Fan, Xiaolin Chang

Abstract—Private inference based on Secure Multi-Party Computation (MPC) addresses data privacy risks in Machine Learning as a Service (MLaaS). However, existing MPC-based private inference frameworks focus on semi-honest or honest majority models, whose threat models are overly idealistic, while malicious security dishonest majority models face the challenge of low efficiency. To balance security and efficiency, we propose a private inference framework using Helper-Assisted Malicious Security Dishonest Majority Model (HA-MSDM). This framework includes our designed five MPC protocols and a co-optimized strategy. These protocols achieve efficient fixed-round multiplication, exponentiation, and polynomial operations, providing foundational primitives for private inference. The co-optimized strategy balances inference efficiency and accuracy. To enhance efficiency, we employ polynomial approximation for nonlinear layers. For improved accuracy, we construct sixth-order polynomial approximation within a fixed interval to achieve high-precision activation function fitting and introduce parameter-adjusted batch normalization layers to constrain the activation escape problem. Benchmark results on LeNet and AlexNet show our framework achieves 2.4-25.7× speedup in LAN and 1.3-9.5× acceleration in WAN compared to state-of-the-art frameworks (IEEE S&P’25), maintaining high accuracy with only 0.04%-1.08% relative errors.

Index Terms—Private inference, polynomial approximation, helper, batch normalization.

I. INTRODUCTION

WITH Artificial intelligence’s (AI) rapid growth, Machine Learning as a Service (MLaaS) enables quick AI model deployment. Users upload data to cloud platforms for model training and inference using robust computational resources. However, this introduces privacy risks as uploaded data may contain sensitive information like medical records or financial data, where leakage could cause severe consequences.

Private inference techniques address this by safeguarding data confidentiality while preserving inference accuracy. Among various solutions [1] [2] for achieving private inference, Secure Multiparty Computation (MPC) [3] stands out as an advanced cryptographic tool enabling collaborative computation over private inputs without revealing them. For example, healthcare institutions can collaboratively perform disease diagnosis inference using their patient data without sharing raw information. MPC enables this through cryptographic techniques, ensuring data privacy while

computing outcomes. However, applying MPC to private inference faces **security and efficiency challenges** that limit practical deployment.

A. Motivation

In terms of security, MPC protocols are categorized by threat models based on adversary capabilities (semi-honest vs. malicious) and corruption degrees (honest vs. dishonest majority). Existing research primarily focuses on semi-honest model [4] [5] [6] and malicious security honest majority model [7] [8]. However, real-world scenarios often involve malicious participants who may collude, forming a dishonest majority malicious security model [9] [10]. Unfortunately, due to enhanced security requirements, limited works exist under this model, with efficiency lagging behind honest majority models by an order of magnitude.

This limitation motivates exploring MPC variants that improve efficiency while strengthening security assumptions. We believe that introducing a semi-honest helper party (e.g., a trusted third-party platform) that does not collude with malicious parties in the malicious security dishonest majority model is a promising MPC variant. We refer to this as the **Helper-Assisted Malicious Security Dishonest Majority Model (HA-MSDM)**. Rather than assuming most parties are honest, it’s more practical to identify a single semi-honest party while allowing most parties to be maliciously corrupted. This design balances security guarantees with efficiency.

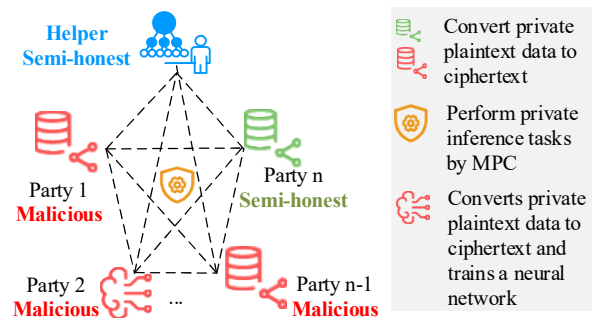


Fig. 1 The MPC-enabled private inference network topology under HA-MSDM

Another critical security consideration is output fairness [11], ensuring all parties either obtain computation results or none do, which provides stronger security guarantees than abort security. In private inference, fairness is particularly critical: if malicious

> REPLACE THIS LINE WITH YOUR MANUSCRIPT ID NUMBER (DOUBLE-CLICK HERE TO EDIT) <

parties can access partial results during the inference process (e.g., intermediate model outputs), these may be exploited to launch model extraction or data reconstruction attacks, posing threats to user privacy. The Asterisk framework [12] first achieves fairness under HA-MSDM, breaking theoretical limitations of traditional MPC protocols. However, the primitive design of Asterisk primarily targets general-purpose computation tasks and lacks sufficient optimization for private inference requirements. We improve and extend Asterisk's cryptographic primitives with specific optimizations for private inference scenarios. **Error! Reference source not found.** illustrates the network topology for private inference implemented with MPC under HA-MSDM model.

In terms of efficiency, while secret-sharing-based MPC protocols efficiently handle addition and multiplication operations [13], the bottleneck in private inference lies in non-linear layers [14] [15], such as activation functions and max-pooling layers. Current solutions include hybrid protocols with costly conversion operations or polynomial approximation approaches. The first approach requires numerous costly protocol conversion operations, resulting in prohibitive time overhead, so our solution adopts polynomial approximation. Nevertheless, this approach confronts two challenges: (1) high-degree polynomial computations requiring sequential execution with linear communication rounds growth; (2) escaping activation problems [16] when inputs exceed fixed intervals, degrading inference accuracy. In our work, we address these challenges by collaboratively optimizing both inference efficiency and accuracy.

B. Our Techniques

To enhance inference efficiency, we optimized Asterisk's multiplication protocol by reducing unnecessary communication overhead in the preprocessing phase. To support fixed-point computation, we merged multiplication and truncation operations, implementing a multiplication-truncation protocol.

For efficient exponentiation, we initially transformed computing x^i into computing $x^{i \cdot r^j}$, where $j = 0$ yields x^i , designing a fast fixed-round integer exponentiation protocol. However, theoretical analysis showed this approach could not extend to fixed-point arithmetic. Consequently, we adopted an alternative strategy leveraging the binomial theorem and parallelization to develop an efficient fixed-round two-party exponentiation protocol.

When extending to fixed-point polynomial computations, we encountered integer overflow issues as polynomial degree increased. We devised a secure restriction strategy confining input to a predefined range, achieving an efficient fixed-round two-party polynomial protocol.

To enhance inference accuracy, we approach the problem from two perspectives: (1) **Constraining escaping activation problem**. While PILLAR [17] implements input constraints through activation regularization and clipping, this may limit model expressiveness and complicate parameter tuning. We find batch normalization (BN) more effective for improving accuracy and systematically analyze parameter selection for BN layers, providing appropriate recommendations. (2) **Accurate fitting within intervals**. Previous research [18] [19] [20] [21]

[22] has been constrained by computational overhead, relying on low-degree polynomial approximations that yield substantial errors and poor inference accuracy, limiting applicability to neural networks with fewer layers. Our efficient primitives enable accurate fitting using relatively high polynomial degrees while maintaining low computational overhead.

C. Our Contributions

We propose the private inference framework in HA-MSDM model. The main contributions are summarized below:

- 1) **Efficient MPC over Arithmetic Circuits**: we constructed efficient MPC protocols over arithmetic circuits in HA-MSDM model, including multiplication, multiplication-truncation, exponentiation, fixed-point two-party exponentiation, and two-party polynomial protocols. Notably, all our protocols can be completed within a fixed number of communication rounds. The main theoretical improvements are summarized in TABLE I.
- 2) **Co-optimized Private Inference Strategy**: We propose a co-optimized private inference strategy. Specifically, we replace nonlinear functions with polynomial approximations to enhance inference efficiency, while introducing a scheme that combines high-order fixed-interval approximation and parameter-adjusted batch normalization to achieve high-precision inference in deep networks. **To the best of our knowledge**, we are the first to address batch normalization parameter selection, providing comprehensive analysis and well-founded recommendations.
- 3) **Implementation and Evaluation**: We implemented our framework in C++ on top of MD-ML framework [9] and conducted extensive evaluations on the LeNet and AlexNet networks under both LAN and WAN settings.

TABLE I

COMPARISON OF THEORETICAL COMMUNICATION COST AND ROUNDS WITH ASTERISK

Operations	Framework	Comm. [elements]	Round
Mult [†]	Ours	2	1
	Asterisk	3	2
Integer Exp [‡]	Ours	$2n$	2
	Asterisk	$2n(k-1)$	$2(k-1)$
Fixed-point Exp for Two Party [‡]	Ours	$10k+2$	4
	Asterisk	$4(k-1)$	$2(k-1)$
Fixed-point Poly for Two Party [‡]	Ours	$8k+12$	4
	Asterisk	$4(k-1)$	$2(k-1)$

[†]: Mult is compared in the preprocessing phase, while other operations are compared in the online phase.

[‡]: n denotes the number of parties, and k represents the maximum degree of exponentiation.

Compared with state-of-the-art dishonest majority maliciously secure private inference framework (MD-SONIC) [10], our framework achieves 2.4-25.7 \times speedup in LAN settings and 1.3-9.5 \times acceleration in WAN settings for NN inference.

D. Organization

In Section II, we introduce related work. In Section III, we

> REPLACE THIS LINE WITH YOUR MANUSCRIPT ID NUMBER (DOUBLE-CLICK HERE TO EDIT) <

present the preliminaries, including notation, threat model, and overview of Asterisk. In Section IV, we specifically introduce the implementation methods of our efficient building blocks and analyze their performance. In Section V, based on the building blocks from Section IV, we propose a complete private inference framework. In Section VI, we present our experimental results. In Section VII, we summarize our work.

II. RELATED WORK

A. Malicious Security Dishonest Majority MPC and Variants

Pure MPC: Damgård et al.'s SPDZ [1], [24] secures MPC via MAC-authenticated shares over finite field \mathbb{F} . MASCOT by Keller et al. [25] replaced costly homomorphic encryption with oblivious transfer, improving SPDZ's offline phase efficiency. Overdrive by Keller et al. [26] enhances preprocessing efficiency by substituting MASCOT's oblivious transfer with additive homomorphic encryption. A breakthrough came with SPDZ_{2k} [27], which extended the SPDZ protocol from finite fields to rings \mathbb{Z}_{2^k} , overcoming the limitation of field-only computation. Overdrive2k [28] adapted Overdrive techniques to \mathbb{Z}_{2^k} by introducing specialized packing techniques for BGV encryption. MD-ML [9] pioneered the extension of TurboSpeedz's circuit-dependent preprocessing to \mathbb{Z}_{2^k} , achieving constant online communication for dot products, and zero-cost truncation operations. MD-SONIC [10] combines SPDZ_{2k} and TinyOT for mixed circuits, cutting binary costs via optimized carry handling and preprocessing.

Variants: To enhance efficiency and security in MPC, researchers have also investigated MPC-model variants. Early works [29] [30] [31] introduced completely honest Helpers with minimal capabilities. [32] first modeled the Helper as semi-honest and non-colluding, achieving strong security guarantees like fairness/GOD but with poor efficiency. [33] considered probabilistic semi-honest Helpers (malicious with finite probability), achieving efficiency but only weak abort security. Asterisk [12] combined both advantages using semi-honest, non-colluding Helpers with efficient primitives to achieve relatively efficient protocols with fairness guarantees. Based on this analysis, we believe implementing private inference under HA-MSDM is reasonable, and currently no existing work has achieved a complete private framework in HA-MSDM. Therefore, we plan to fill this gap.

B. Polynomial Approximation in Nonlinear Layer

[18], [19] implement low-precision shallow network inference using sub-quadratic polynomials, with [19] adding BN layers for improved accuracy but remaining depth-limited. [20] provides refined polynomial approximation and replaces max pooling with average pooling but achieves limited accuracy. [21] proposes a mixed protocol using a planner to select between garbled circuits (GC) and polynomial computation for ReLUs, requiring meticulous parameter tuning and incurring substantial GC overhead. [34] uses ultra-high degree polynomials (29th degree) for precise approximation but with unbearable computational cost. The most advanced works are [16] and [17]. [16] first systematically identifies the

escaping activation problem in deep networks and proposes approximate min-max normalization, but suffers significant accuracy degradation with increased depth. [17] introduces activation regularization and clipping for deep network inference with sufficient accuracy, but constrains model expressiveness and doesn't improve training convergence or accuracy. Therefore, we adopt polynomial fitting with BN layers before activation functions, considering fixed-point polynomial fitting, and first achieve deep network inference by adjusting BN layer coefficients.

III. PRELIMINARIES

A. Notation

In this section, we present the notation used in this paper. While the Asterisk implements circuit-dependent preprocessing in finite field \mathbb{F} , we adapt this to operate over ring \mathbb{Z}_{2^l} for two reasons: (1) more efficient CPU computation in \mathbb{Z}_{2^l} , and (2) simpler design and implementation of private inference operations (e.g., truncation and comparison). In computing, we consider two data types: integers and fixed-point numbers, both represented using signed two's complement in \mathbb{Z}_{2^l} where the most significant bit is the sign bit. They differ in bit allocation: integers use remaining bits for the integer part, while fixed-point numbers allocate d least significant bits for the fractional part.

For sharing semantics, we adopt Asterisk's formulation. For secret value $x \in \mathbb{Z}_{2^l}$, we establish additive secret-sharing where $x = \sum_{i=1}^n [x]_i$, with each participant P_i maintaining fragment $[x]_i$. Authentication uses information-theoretic MAC under global key $\Delta \in \mathbb{Z}_{2^l}$, where the authentication tag t_x for value x is computed as $t_x = x \cdot \Delta$, with both t_x and Δ being additively secret-shared. Below we present three sharing semantics used in our work, with TABLE II summarizing the corresponding notations used throughout this paper:

- **Additive Sharing:** Value $x \in \mathbb{Z}_{2^l}$ is additively shared among n participants $\{P_1, \dots, P_n\}$ if each participant P_i possesses a fragment $[x]_i \in \mathbb{Z}_{2^l}$, such that $x = \sum_{i=1}^n [x]_i$.
- **MAC Sharing:** Value $x \in \mathbb{Z}_{2^l}$ is MAC-shared among participants if each participant P_i holds a pair $\langle x \rangle_i = ([x]_i, [t_x]_i)$, such that $t_x = x \cdot \Delta$.
- **Masked Sharing:** Value $x \in \mathbb{Z}_{2^l}$ is mask-shared among participants if each participant holds a pair $[[x]]_i = (m_x, \langle \delta_x \rangle_i)$, where $\delta_x \in \mathbb{Z}_{2^l}$ is a random mask, such that $m_x = x + \delta_x$.

TABLE II
NOTATION USED THROUGHOUT THIS PAPER

$[1, n]$	The set of integers $\{1, 2, \dots, n\}$
P_1, P_2, \dots, P_n	n parties in the secure computation
HP	The semi-honest helper party

> REPLACE THIS LINE WITH YOUR MANUSCRIPT ID NUMBER (DOUBLE-CLICK HERE TO EDIT) <

$[x]$	The set of additive sharing for value x
$\langle x \rangle$	The set of masked sharing for value x
$[[x]]$	The set of MAC sharing for value x
$\overline{x_n}$	The vector with elements (x_1, x_2, \dots, x_n)
δ_x	The plaintext masking value of value x
Δ	The global MAC key
t_x	The authentication tag of value x , computed as
m_x	The masked value of value x , computed as
l	The bit-length of elements in \mathbb{Z}_{2^l}
d	The number of fractional bits in fixed-point

Note that: Subscript i in $[x]_i$, $\langle x \rangle_i$, $[[x]]_i$ denotes the share of value x held by the i -th party P_i in additive, MAC, masked sharing schemes

B. Threat Model

In this section, we introduce the threat model used in the paper, namely HA-MSDM, and describe the capabilities of the parties, the HP, and the attackers.

We consider a distributed computation system comprising n parties denoted by $P = \{P_1, \dots, P_n\}$. Each party P_i is provisioned with private input $x_i \in \{0, 1\}^*$ and independent randomness $r_i \in \{0, 1\}^*$. The computation proceeds in synchronous rounds, where parties communicate through a fully connected network with private and authenticated point-to-point channels. The system incorporates an auxiliary entity, referred to as Helper (HP), which exists outside the set of computing parties P . HP maintains a secure communication channel with each party P_i , ensuring both privacy and authentication. A distinguishing characteristic of the HP is that it neither possesses initial inputs nor receives final outputs from the protocol execution. HP is permitted to be stateful, meaning that HP is allowed to retain intermediate results generated during interaction rounds with parties.

For attackers, we consider a non-colluding adversary model, which means the adversary can either maliciously corrupt $n-1$ out of n parties, or semi-honestly corrupt HP. We emphasize that the adversary is non-colluding, meaning that a semi-honest adversary is not permitted to obtain the view of a malicious adversary. This represents the fundamental distinction in adversarial capabilities between HA-MSDM and FaF (friends-and-foes) security model [35].

C. Overview of Asterisk

This section introduces Asterisk's construction and key components to facilitate understanding of our building blocks. Asterisk consists of three main phases:

- 1) **Setup Phase:** The fundamental purpose is to establish shared keys among parties and HP. Through shared keys, combined with secure pseudorandom functions (PRFs) and local counters, multiple parties generate identical secret values without interaction, crucial for preprocessing mask generation. Specifically, each party P_i maintains common key k_i with HP, the set of parties P maintain common key k_p , and global key k_{all} is established between parties P and HP.

- 2) **Preprocess Phase:** The preprocessing phase is input-independent and can be executed once the computation circuit is determined. For semi-honest secure MPC, preprocessing generates mask value shares on each wire. For malicious MPC, it additionally generates MAC-multiplied mask shares for verification. This concept is equally applicable in Asterisk. Unlike traditional MPC, Asterisk allows HP to know plaintext mask values for each wire. Leveraging this, Asterisk developed three efficient functions for rapidly generating MAC sharing for different secret types, which are also used in our efficient building blocks. We introduce only the functionality and communication complexity without implementation details.

- a) $\mathcal{F}_{(\cdot)-sh}(P_d, Rand)$: generates a MAC sharing of a random value known to the dealer P_d and HP with a communication cost of two ring elements.
- b) $\mathcal{F}_{(\cdot)-sh}(HP, Rand)$: generates a MAC sharing of a random value known to HP with a communication cost of one ring element.
- c) $\mathcal{F}_{(\cdot)-sh}(HP, v)$: generates a MAC sharing of v held by HP with a communication cost of two ring elements.
- 3) **Online Phase:** The online phase is used to execute the specific computational tasks after all parties input their data. We represent computational tasks using gate circuits with three gate types:
 - a) Input Gate: The purpose of this gate is to transform the input value x into its masked sharing $[[x]]$.
 - b) Computation Gates: Assuming the function to be computed is $y = f(x_1, \dots, x_p)$, the computation gates take as input the shared values $[[x_1]], \dots, [[x_p]]$ and produce the shared output $[[y]]$. These gates perform the actual secure computation on the shared representations without revealing the underlying values.
 - c) Output Gate: This gate executes the reverse process of the input gate, converting the shared representation $[[y]]$ back to its plaintext value y , thereby revealing the final computation result to the designated parties.

Our work focuses on improving existing computation gates, designing novel and efficient computation gates, and developing a complete private inference framework.

IV. EFFICIENT BUILDING BLOCKS

This section introduces our efficient MPC building blocks: (Section IV-A) multiplication protocol, (Section IV-B) multiplication-with-truncation protocol, (Section IV-C) multi-party exponentiation protocol, (Section IV-D) two-party exponentiation protocol, and (Section IV-E) two-party polynomial protocols. We analyze our building blocks' advantages over state-of-the-art MPC schemes regarding time complexity, communication overhead, and communication rounds.

A. Multiplication Protocol

A multiplication protocol refers to the process that takes input wires x and y and output wire z , computing

> REPLACE THIS LINE WITH YOUR MANUSCRIPT ID NUMBER (DOUBLE-CLICK HERE TO EDIT) <

$[[z]] = [[x \cdot y]]$ from the input wire values $[[x]]$ and $[[y]]$. In Asterisk, the multiplication protocol invokes $\mathcal{F}_{(\cdot)-sh}(HP, Rand)$ once to generate MAC sharing of the mask δ_z for the output wire z , and invokes $\mathcal{F}_{(\cdot)-sh}(HP, v)$ once to generate the MAC sharing of $\delta_x \cdot \delta_y$ in the preprocess phase, which is the product of input wire mask value, and obtains the output wire value $[[z]] = (m_z, \langle \delta_z \rangle)$ by executing Equation (1) in the online phase.

$$\begin{aligned} m_z &= z + \delta_z = x \cdot y + \delta_z \\ &= (m_x - \delta_x) \cdot (m_y - \delta_y) + \delta_z \\ &= m_x \cdot m_y - m_x \cdot \delta_y - m_y \cdot \delta_x + \delta_x \cdot \delta_y + \delta_z \end{aligned} \quad (1)$$

In the preprocessing phase, the main purpose of the protocol is to enable each party to generate masked sharing of the mask values on each wire, where the helper is allowed to know the plaintext mask values on the wires. In the online phase, the main purpose of the protocol is to generate the sum of the plaintext wire values and the plaintext mask values, where the helper is not allowed to know this value. Therefore, inspired by these ideas, we observe that invoking $\mathcal{F}_{(\cdot)-sh}(HP, Rand)$ in Asterisk's multiplication protocol is unnecessary. We can make $\delta_z = \delta_x \cdot \delta_y$ and invokes $\mathcal{F}_{(\cdot)-sh}(HP, v)$ once to generate the MAC sharing of δ_z . The intuitive idea is that when at least one party is honest, an adversary knowing $\langle \delta_x \rangle$, $\langle \delta_y \rangle$, $\langle \delta_x \cdot \delta_y \rangle$ cannot obtain any of the values $\delta_x, \delta_y, \delta_x \cdot \delta_y$.

Protocol 1: Π_{mult}

Preprocessing phase:

For a gate with inputs $[[x]]$ and $[[y]]$, HP knows $\delta_x, \delta_y, \langle \delta_x \rangle, \langle \delta_y \rangle$, parties know $\langle \delta_x \rangle$ and $\langle \delta_y \rangle$.

1. HP computes $\delta_{xy} = \delta_x \cdot \delta_y$ and gets the output wire mask value $\delta_z = \delta_{xy}$.
 2. All parties and HP execute $\mathcal{F}_{(\cdot)-sh}(HP, \delta_{xy})$ to generate $\langle \delta_{xy} \rangle$.
-

Online phase:

Input: P_i has $\langle \delta_{xy} \rangle_i, [[x]]_i, [[y]]_i$, HP has $\delta_x, \delta_y, \delta_{xy}$.

Output: For $i \in [1, n]$, P_i 's output $m_z = z + \delta_{xy}$, where $z = x \cdot y$.

Protocol:

1. For $i \in [1, n]$, P_i computes $[t_{m_z}]_i = [\Delta]_i \cdot m_x \cdot m_y - m_x \cdot [t_{\delta_y}]_i - m_y \cdot [t_{\delta_x}]_i + 2 \cdot [t_{\delta_{xy}}]_i$.
 2. P_1 computes and sends $[m_z]_1$ to P_{king} , where $[m_z]_1 = m_x \cdot m_y - m_x \cdot [\delta_y]_1 - m_y \cdot [\delta_x]_1 + 2 \cdot [\delta_{xy}]_1$.
 3. For $i \in [1, n] / \{1\}$, P_i computes and sends $[m_z]_i$ to P_{king} , where $[m_z]_i = -m_x \cdot [\delta_y]_i - m_y \cdot [\delta_x]_i + 2 \cdot [\delta_{xy}]_i$.
 4. P_{king} reconstructs m_z and sends it to all parties excluding HP.
 5. For $i \in [1, n]$, P_i 's output $[[z]]_i = (m_z, \langle \delta_z \rangle_i)$.
-

B. Multiplication-with-truncation Protocol

Private inference operations involve decimals. We convert floating-point to fixed-point format during input, perform fixed-point arithmetic throughout computation, and convert back to floating-point in output. In fixed-point arithmetic, each multiplication operation doubles the number of fractional bits. To prevent fractional bits from encroaching on integer bits and causing overflow, multiplication results must be truncated by discarding the last d bits.

Assume we have an input $[[x]] = (m_x, \langle \delta_x \rangle)$, where $m_x = x + \delta_x$. The essence of the truncation operation is to generate $[[x / 2^d]] = (m'_x, \langle \delta'_x \rangle)$, where $m'_x = x / 2^d + \delta'_x$. Hence, we recognize that the key to successful truncation lies generating MAC sharing of mask value in the preprocessing phase and performing the truncation operation on m_x in the online phase. The protocol $\Pi_{mult-Trun}$ is presented below.

Protocol 2: $\Pi_{mult-Trun}$

Preprocessing phase:

For a gate with inputs $[[x]]$ and $[[y]]$, HP knows $\delta_x, \delta_y, \langle \delta_x \rangle, \langle \delta_y \rangle$, parties know $\langle \delta_x \rangle$ and $\langle \delta_y \rangle$.

1. HP and parties execute preprocessing phase of Π_{mult} . Parties obtain $\langle \delta_{xy} \rangle$ and HP generate the mask value δ_{xy} .
 2. HP computes $\delta_{xy}' = \delta_{xy} / 2^d$ and gets the output wire mask value $\delta_z' = \delta_{xy}'$ and $\delta_z = \delta_{xy}$.
 3. All parties and HP execute $\mathcal{F}_{(\cdot)-sh}(HP, \delta_{xy}')$ to generate $\langle \delta_{xy}' \rangle$.
-

Online phase:

Input: P_i has $\langle \delta_{xy} \rangle_i, \langle \delta_{xy}' \rangle_i, [[x]]_i, [[y]]_i$, HP has $\delta_x, \delta_y, \delta_{xy}, \delta_{xy}'$.

Output: For $i \in [1, n]$, P_i 's output

$$m_z' = z' + \delta_z' = z / 2^d + \delta_{xy}' = (x \cdot y) / 2^d + \delta_{xy}'.$$

Protocol:

1. HP and Parties execute the online phase of Π_{mult} . For $i \in [1, n]$, P_i gets $[[z]]_i$.
 2. For $i \in [1, n]$, P_i computes $m_z' = m_z / 2^d$ and outputs $[[z']]_i = (m_z', \langle \delta_z' \rangle_i)$.
-

Correctness: We establish the correctness of $\Pi_{mult-Trun}$ through the following proposition.

Proposition: In the protocol $\Pi_{mult-Trun}$, when processing fixed-point numbers x and y satisfying $x \cdot y \leq 2^k$ (where k represents the bit-length of elements in the integer ring \mathbb{Z}_{2^k}), the following probabilistic outcomes govern the result:

1. With probability P , where

> REPLACE THIS LINE WITH YOUR MANUSCRIPT ID NUMBER (DOUBLE-CLICK HERE TO EDIT) <

$P = \Pr[(x \cdot y \bmod 2^d) + (\delta_x \cdot \delta_y \bmod 2^d) < 2^d]$, the truncated value m_z' is computed as $z' + \delta_z'$.

- Conversely, with probability $1 - P$, the result requires an additive correction: $m_z' = z' + \delta_z' + 1$.

C. Multi-party Exponentiation Protocol

We present an efficient multi-party exponentiation protocol, where given an input $[[x]]$, the protocol outputs $[[x^i]]$ for $i \in [1, k]$, k represents the highest power.

A naive approach would execute k sequential Π_{mult} , storing each intermediate result. However, this suffers from a critical limitation: each subsequent multiplication (computing $[[x^i]]$) depends on the output of previous multiplication ($[[x^{i-1}]]$), forcing $O(k)$ communication rounds during online phase. In contrast, our optimized multi-party exponentiation protocol achieves **two key advantages**: 1) The protocol supports arbitrary number of parties without compromising efficiency, 2) online communication requires only 2 rounds, independent of the exponent k . **To the best of our knowledge**, no prior work in HA-MSDM model has achieved similar results.

Specifically, inspired by the work of Lu et al. [36], we transform the problem of computing $[[x^i]]$ into calculating $[[x^i \cdot r^j]]$ through factorization, where r is a random number generated by HP. We further optimize the iterative Equation (2), where $x - r$ represents a publicly known constant value shared among all parties but kept secret from HP. By employing dynamic programming, we ultimately obtain $[[x^i]]$ once $[[x^i \cdot r^0]]$ is computed. The protocol $\Pi_{mult-exp}$ is presented below.

$$x^i \cdot r^j = (x - r) \cdot x^{i-1} \cdot r^j + x^{i-1} \cdot r^{j+1} \quad (2)$$

Protocol 3: $\Pi_{mult-exp}$

Preprocessing phase:

For a gate with inputs $[[x]]$, output $[[x]]$, $[[x^2]]$, ..., $[[x^k]]$.

- HP and parties execute k times of $\mathcal{F}_{\langle \cdot \rangle-sh}(HP, Rand)$ to generate $\langle \delta_r \rangle$, $\langle \delta_{r^2} \rangle$, ..., $\langle \delta_{r^k} \rangle$.
- HP instantiates a random number r , computes r^2 , r^3 , ..., r^k , and computes $m_{r^i} = r^i + \delta_{r^i}$, where $i \in [1, k]$, and sends to all of parties.
- Parties reconstruct $[[r^i]]$, where $i \in [1, k]$.

Online phase:

Input: P_i has $[[r]]_i$, $[[r^2]]$, ..., $[[r^k]]$, $[[x]]$, HP has δ_x , δ_r , ..., δ_{r^k} , r .

Output: For $i \in [1, n]$, P_i 's output $[[x]]_i$, $[[x^2]]_i$, ..., $[[x^k]]_i$.

Protocol:

- Parties instantiate a random number b by k_p , and compute locally $q_x = m_x + b = x + \delta_x + b$, and send q_x

to HP.

- HP checks whether all messages are identical. If not, the protocol terminates; otherwise, it proceeds.
- HP computes $q_x - r - \delta_x = x + b - r$ and sends it to all parties.
- All parties compute $c = x + b - r - b = x - r$.
- All parties initialize $arr[k+1][k+1]$ (where $arr[i][j]$ will store $[[x^i \cdot r^j]]$) and execute the following procedure.

- for($i = 1; i \leq k; i++$) { $arr[0][i] = [[r^i]]$;
- $arr[1][0] = [[x]]$;
- for($i = 1; i < k; i++$)
- for($j = 1; j \leq k - i; j++$)
- $arr[i][j] = c \cdot arr[i-1][j] + arr[i-1][j+1]$;
- for($i = 2; i \leq k; i++$)
- $arr[i][0] = c \cdot arr[i-1][0] + arr[i-1][1]$;

- All parties get $[[x^i]] = arr[i][0]$.

D. Two-party Exponentiation Protocol

While $\Pi_{mult-exp}$ is efficient for integer exponentiation, it faces challenges with fixed-point exponentiation because each multiplication in fixed-point arithmetic requires truncation to prevent fractional overflow. Specifically, in the $\Pi_{mult-exp}$, we employ Equation (3) to compute $[[x^i \cdot r^j]]$, where $[[x^i \cdot r^j]] = (m_{x^i r^j}, \langle \delta_{x^i r^j} \rangle)$, but computing $c \cdot \langle \delta_{x^i r^j} \rangle / 2^d$ is not permitted because for any integer x , $\sum_{i=1}^n ([x]_i / 2^d) \neq x / 2^d$. Hence, $\sum_{k=1}^n ([\delta_{x^i r^j}]_k / 2^d) \neq \delta_{x^i r^j} / 2^d$ will ultimately lead to incorrect computation results.

$$[[x^i \cdot r^j]] = c \cdot [[x^{i-1} \cdot r^j]] + [[x^{i-1} \cdot r^{j+1}]] \quad (3)$$

To enable exponentiation for fixed-point computations while preserving constant-round communication, we adopt a fundamentally different approach to design a two-party exponentiation protocol inspired by Diaa et al [17]. Specifically, we leverage the binomial theorem (4) to transform x^k computation into summing terms $x_1^i \cdot x_2^{k-i}$, where $x = x_1 + x_2$. Fig. 2 illustrates the computational workflow for deriving $[[x^k]]$ from $[[x]]$. To simultaneously compute all $[[x^i]]$ where $i \in [1, k]$, one only needs to execute identical workflows in parallel. The protocol $\Pi_{two-exp}$ is presented below. Π_{input} and $\Pi_{dot-product}$ are explained in the supplementary file.

> REPLACE THIS LINE WITH YOUR MANUSCRIPT ID NUMBER (DOUBLE-CLICK HERE TO EDIT) <

TABLE III
USING $\Pi_{\text{mult-exp}}$, $\Pi_{\text{two-exp}}$, Π_{mult} TO COMPUTE $[[x^k]]$ FROM $[[x]]$

	$\Pi_{\text{mult-exp}}$	$\Pi_{\text{two-exp}}$	Π_{mult}
(1)	$k(n+1)$	$4k$	$2(k-1)$
(2)	$2n$	$10k+2$	$2n(k-1)$
(3)	2	4	$2(k-1)$

$$x^k = (x_1 + x_2)^k = \sum_{i=0}^k C_k^i \cdot x_1^i \cdot x_2^{k-i} \quad (4)$$

Protocol 4: $\Pi_{\text{two-exp}}$

Preprocessing phase:

For a gate with input $[[x]]$, HP knows δ_x , parties know $\langle \delta_x \rangle$.

1. HP and parties invoke $\mathcal{F}_{(\cdot)-sh}(HP, \text{Rand})$ $2k+2$ times, with HP obtaining $\delta_{x_1^0}, \delta_{x_1^1}, \dots, \delta_{x_1^k}, \delta_{x_2^0}, \delta_{x_2^1}, \dots, \delta_{x_2^k}$ and parties obtaining $\langle \delta_{x_1^0} \rangle, \langle \delta_{x_1^1} \rangle, \dots, \langle \delta_{x_1^k} \rangle, \langle \delta_{x_2^0} \rangle, \langle \delta_{x_2^1} \rangle, \dots, \langle \delta_{x_2^k} \rangle$.
2. Subsequently, HP computes $\delta_{x^i} = C_k^i \cdot \delta_{x_1^i} \cdot \delta_{x_2^{k-i}}$, where $i \in [0, k]$.
3. HP and parties invoke $\mathcal{F}_{(\cdot)-sh}(HP, v)$ $k+1$ times, with parties obtaining $\langle \delta_{x^i} \rangle$, where $i \in [0, k]$.

Online phase:

Input: P_i has $[[x]]$, $\langle \delta_{x_1^i} \rangle_i, \langle \delta_{x_2^i} \rangle_i, \langle \delta_{x^i} \rangle$, where $j \in [0, k]$.

Output: For $i \in [1, n]$, P_i 's output $[[x^j]]_i$, where $j \in [0, k]$.

Protocol:

1. P_1 computes $x_1 = m_x - [\delta_x]_1$ and gets x_1^j , where $j \in [0, k]$.
2. P_2 computes $x_2 = -[\delta_x]_2$ and gets x_2^j , where $j \in [0, k]$.
3. Parties execute $2(k+1)$ times of Π_{input} 's online phase to obtain $([[x_1^j]], [[x_2^j]])$ in parallel, where $j \in [0, k]$.
4. Parties execute scalar multiplication to compute $C_q^j \cdot [[x_1^j]]$, where $q \in [0, k]$, $j \in [0, k]$.
5. Parties reverse the order of $[[x_2^j]]$, where $j \in [0, k]$.
6. Parties execute $k+1$ times of $\Pi_{\text{dot-product}}$'s online phase to obtain $[[x^j]]$ in parallel, where $j \in [0, k]$.

E. Two-party Polynomial Protocol

For nonlinear layers, we employ polynomial approximation, making efficient polynomial protocols essential. Since machine learning primarily involves fractional data, polynomial protocols supporting only integer arithmetic are insufficient. Our solution implements fixed-point polynomial computation.

We present a specialized two-party polynomial protocol for activation function computation, constructed upon our two-party exponentiation protocol $\Pi_{\text{two-exp}}$.

Specifically, since activation functions are typically executed after data normalization and clipping operations, their inputs generally fall within a fixed interval. Assuming the activation function's input domain is $[-q, q]$, we execute the following operations:

1. Randomly select x_1 from the uniform distribution over $[-q \cdot 2^d, q \cdot 2^d]$.
2. Ensure x is a fixed-point value within $[-q \cdot 2^d, q \cdot 2^d]$.
3. By the constraint $x_1 + x_2 = x$, it follows that x_2 must lie within $[-2q \cdot 2^d, 2q \cdot 2^d]$.

Rationale for Value Constraints: Restricting x_1 and x_2 to these ranges is critical because it prevents integer overflow during subsequent exponentiation operations—a fundamental requirement for the correctness of polynomial protocols.

Furthermore, we must convert polynomial coefficients to fixed-point representation and apply unified truncation to maintain numerical precision. For notational clarity, we adopt a fixed-point representation where both input value x and polynomial coefficients a_i are scaled by 2^d , expressed as $x = x' \cdot 2^d$ and $a_i = a_i' \cdot 2^d$, where $i \in [0, k]$. x' denotes the original input value and a' denotes the true polynomial coefficients in unscaled form. The protocol $\Pi_{\text{two-poly}}$ is presented below.

Protocol 5: $\Pi_{\text{two-poly}}$

Preprocessing phase:

For a gate with input $[[x]]$, HP knows δ_x , parties know $\langle \delta_x \rangle$.

1. HP and parties execute preprocessing phase of $\Pi_{\text{two-exp}}$.
2. HP computes $\delta_y = \sum_{j=0}^k a_j \cdot \sum_{i=0}^j C_j^i \cdot \delta_{x_1^i} \cdot \delta_{x_2^{j-i}}$ and $\delta_y' = \delta_y / 2^d$.

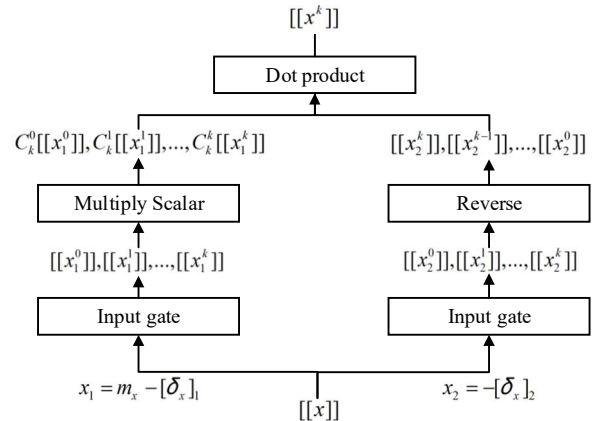


Fig. 2. $\Pi_{\text{two-exp}}$ computes $[[x^k]]$ from $[[x]]$.

> REPLACE THIS LINE WITH YOUR MANUSCRIPT ID NUMBER (DOUBLE-CLICK HERE TO EDIT) <

- HP and parties execute $\mathcal{F}_{\langle \cdot \rangle-sh}(HP, \delta_y')$ to generate $\langle \delta_y' \rangle$.

Online phase:

Input: For $i \in [1, n]$, P_i has $[[x]]$, $\langle \delta_y' \rangle$, $(\langle \delta_{x_i} \rangle_i, \langle \delta_{x_i'} \rangle_i)$, where $j \in [0, k]$.

Output: For $i \in [1, n]$, P_i 's output $[[y']] = (m_y', \langle \delta_y' \rangle)$,

where $y' = y / 2^d = (\sum_{i=0}^k a_i \cdot x^i / 2^{d(i-1)}) / 2^d$.

Protocol:

- P_1 computes $\tilde{x}_1 = m_x - [\delta_x]_1$ and generates a random value $x_1 \in [-q \cdot 2^d, q \cdot 2^d]$ and gets $x_1^j / 2^{d(j-1)}$, where $j \in [0, k]$.
- P_1 computes $dist = \tilde{x}_1 - x_1$ and send it to p_2 .
- P_2 computes $\tilde{x}_2 = -[\delta_x]_2$, $x_2 = \tilde{x}_2 + dist$ and gets $x_2^j / 2^{d(j-1)}$, and reverses the order of $x_2^j / 2^{d(j-1)}$ where $j \in [0, k]$.
- Parties execute $2(k+1)$ times of Π_{input} 's online phase to obtain $([[x_1^j / 2^{d(j-1)}]], [[x_2^j / 2^{d(j-1)}]])$ in parallel, where $j \in [0, k]$.
- Parties execute scalar multiplication to compute $[[a_q \cdot C_q^j \cdot x_1^j / 2^{d(j-1)}]]$, where $q \in [0, k]$, $j \in [0, q]$.
- Parties only need to execute $\Pi_{dot-product}$'s online phase once to obtain $[[y]]$, where $y = \sum_{j=0}^k a_j \cdot x^j / 2^{d(j-1)}$.
- For $i \in [1, n]$, P_i computes $m_y' = m_y / 2^d$ and outputs $[[y']]_i = (m_y', \langle \delta_y' \rangle_i)$.

Note that: The polynomial protocol requires only a single invocation of $\Pi_{dot-product}$'s online phase. **Fig. 3** explicitly illustrates both the input vectors and output of the dot product protocol implementation.

V. BUILDING A PRIVATE INFERENCE MODEL

In this section, we present a framework for constructing private inference models using fundamental building blocks, where private inference is performed using fixed-point arithmetic by default. Our primary focus centers on CNN architectures, which principally consist of convolution layers, pooling layers, activation function layers, fully connected layers, batch normalization layers.

A. Convolution & Fully connected Layers

Both convolutional and fully connected layers are linear operations. Convolution layers can be viewed as dot product operations between input matrix and convolution kernel. Fully connected layers are intrinsically matrix multiplications. Assuming we have the functions:

- $\mathcal{F}_{conv}(matrix, kernel, params)$: Computes convolution between *matrix* and *kernel*, where *params* denotes configuration parameters.

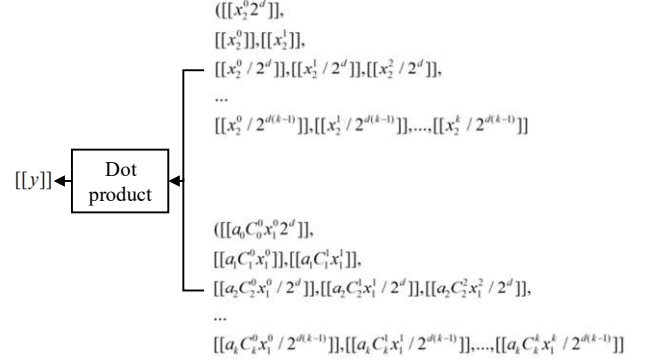


Fig. 3. $\Pi_{dot-product}$'s input and output in $\Pi_{two-poly}$.

TABLE IV
USING $\Pi_{two-poly}$, $\Pi_{mult-trun}$, TO COMPUTE $[[y']]$ FROM $[[x]]$, WHERE $y' = y / 2^d = (\sum_{i=0}^k a_i \cdot x^i / 2^{d(i-1)}) / 2^d$

	$\Pi_{two-poly}$	$\Pi_{mult-trun}$
(1)	$4k+6$	$4k-2$
(2)	$8k+12$	$4(k-1)$
(3)	4	$2(k-1)$

- $\mathcal{F}_{matrix_mult}(input_x, input_y)$: Performs matrix multiplication between *input_x* and *input_y*.

By extending $\Pi_{mult-trun}$, we can securely implement both convolution and fully connected layers. Specifically, when adapting $\Pi_{mult-trun}$ for matrix inputs, we modify only the multiplication operation in Equation (1):

- $\mathcal{F}_{conv}(matrix, kernel, params)$ is used to replace multiplication to yield secure convolution protocol Π_{conv} .
- $\mathcal{F}_{matrix_mult}(input_x, input_y)$ is used to replace multiplication to yield secure fully connected protocol $\Pi_{fully_connect}$.

B. Pooling Layers

We examine two prevalent pooling operations: **average pooling** and **max pooling**, which are fundamentally distinct—the former is nonlinear while the latter is linear.

Average pooling involves summing all matrix elements and dividing by matrix size, with the critical challenge being the division operation. Unlike truncation operations where division by 2^d is efficiently implemented through bit-shifting, we address division by matrix size through fixed-point conversion by precomputing $2^d \cdot 1.0 / matrix.size()$ as a fixed-point constant and subsequently performing secure scalar multiplication-truncation operation. This approach maintains computational efficiency while ensuring numerical precision in the privacy-preserving setting.

For max pooling, our protocol adheres to the methodology outlined in [10], wherein the ReLU function computation is implemented using $\Pi_{two-poly}$. The fundamental component of the max pooling operation is the selection of the maximum

> REPLACE THIS LINE WITH YOUR MANUSCRIPT ID NUMBER (DOUBLE-CLICK HERE TO EDIT) <

value between two elements. We employ the ReLU function to implement this functionality, with the specific operation as delineated in Equation (5). Furthermore, we utilize a binary tree structure to parallelize the comparison operations, achieving the max pooling operation with a circuit depth of $\log_2 n$, where n represents the number of input elements.

$$\text{Max}(a, b) = \text{ReLU}(a - b) + b \quad (5)$$

Furthermore, our framework adopts the optimization strategy from [20], which reverses the positions of Maxpool and ReLU operations during the inference phase, specifically replacing the sequence $\text{BN} \rightarrow \text{ReLU} \rightarrow \text{Maxpool}$ with $\text{BN} \rightarrow \text{Maxpool} \rightarrow \text{ReLU}$. This operation significantly reduces the number of ReLU computations.

C. Batch Normalization Layers

In standard neural network architectures, BN layers are normally positioned prior to activation functions to accelerate training convergence and enhance model accuracy. In our framework, BN layer serves two critical roles beyond accelerating convergence and improving accuracy: (1) By constraining the input to the activation function within a specific range, it enables precise polynomial fitting of the activation function and mitigates the activation escape problem; (2) To ensure computational accuracy, $\Pi_{\text{two-poly}}$ imposes strict requirements on the input range of the activation function, BN layer effectively restricts the input to the prescribed range.

Specifically, we implement BN layers using Equation (6), where μ represents the batch mean, σ^2 represents the batch variance, and ε is a small constant introduced to prevent division by zero or numerical overflow. Through careful adjustment of the scale (γ) and shift (β) parameters, we constrain the normalized input data to the range $[-3\gamma + \beta, 3\gamma + \beta]$. Note that, compared to private training, the implementation of BN layers in private inference is significantly simpler. During inference, the mean and variance are treated as private inputs from one participating party, eliminating the need for complex operations such as square root and division. As a result, the BN layer can be approximated using element-wise matrix multiplication.

$$y = \gamma \cdot \frac{x - \mu}{\sqrt{\sigma^2 + \varepsilon}} + \beta \quad (6)$$

Selection of parameters: We observed that simply adding BN layers is insufficient. In our experiments, precise function approximation could only be achieved within a specific interval. To enable high-precision inference, two key conditions must be satisfied:

- 1) The constraint interval of BN layers should be equal to or slightly larger than the accurate fitting interval of the approximating polynomials. We need to ensure that inputs to activation functions fall within the polynomial accurate fitting interval as much as possible.
- 2) The constraint interval of BN layers should be neither too small nor too large. If too small, taking ReLU as an example, it exhibits a non-differentiable point at $x = 0$, leading to significant approximation errors in polynomial fitting within a small neighborhood around zero.

Moreover, in fixed-point representation, smaller intervals result in fewer representable values, causing larger relative errors between fixed-point and true values. Conversely, if the interval is too large, it becomes challenging to fit activation functions accurately, making it difficult to achieve high-precision fitting with low-degree polynomials.

In all evaluations, the selected parameters are $\gamma = 1.67$ and $\beta = 0$.

D. Activation Function Layers

In our framework, activation function computation is implemented through two distinct approaches based on participant count:

- For two-party scenarios, we employ $\Pi_{\text{two-poly}}$ utilizing least squares approximation to derive optimal coefficients by minimizing mean squared error between the original activation function and its polynomial approximation, followed by redistributing secret-shared intervals to ensure computational correctness within $\Pi_{\text{two-poly}}$.
- For multi-party settings ($n > 2$), we adopt $\Pi_{\text{mult-Trim}}$ to implement polynomial calculation.

We primarily consider ReLU as the activation function and employ the least squares method to achieve precise approximation within the interval $[-5, 5]$. All polynomial coefficients are represented using fixed-point notation, and the mean squared error (MSE) is adopted as the metric to evaluate the fitting accuracy. We observed that when the polynomial degree is set to 6, MSE reaches 0.0036, achieving an optimal balance between approximation accuracy and computational overhead. The polynomial used in all evaluations is:

$$y = 0.0002288818359375x^6 - 0.01124572753906250x^4 + 0.2304840087890625x^2 + 0.5x + 0.213836669921875$$

VI. EXPERIMENTS

A. Experimental Setup

We implemented our protocols in C++20, building upon the MD-ML [9] codebase. The experiments were conducted on a high-performance server running Ubuntu 20.04.5 LTS with a 2.2GHz AMD Ryzen Threadripper 3970X 32-Core Processor (64 logical cores) and 251GB RAM. Our implementation provides a complete simulation of our framework, including all three phases: Setup, Preprocessing, and Online, with full participant interaction and computation processes.

Network simulation: We employed the Traffic Control tool to emulate both WAN and LAN environments with the following parameters:

> REPLACE THIS LINE WITH YOUR MANUSCRIPT ID NUMBER (DOUBLE-CLICK HERE TO EDIT) <

TABLE V
COMPUTATIONAL AND COMMUNICATION OVERHEADS OF Π_{mult} COMPARED TO $\Pi_{Asterisk-mult}$

Operations	The number of participants	LAN		WAN		Total communication	
		Preprocess	Online	Preprocess	Online	Preprocess	Online
Π_{mult}	2	10ms	13ms	143ms	1066ms	1MB	1MB
	3	10ms	14ms	144ms	1468ms	1MB	2MB
	4	10ms	20ms	145ms	1921ms	1MB	3MB
	5	11ms	25ms	146ms	2458ms	1MB	4MB
$\Pi_{Asterisk-mult}$	2	20ms	13ms	184ms	1087ms	1.5MB	1MB
	3	19ms	14ms	185ms	1470ms	1.5MB	2MB
	4	19ms	21ms	186ms	1925ms	1.5MB	3MB
	5	20ms	25ms	187ms	2455ms	1.5MB	4MB

TABLE VI
THE ONLINE COSTS OF NN BUILDING BLOCKS

Operations	Framework	LAN	WAN	Total communication
CONV _{28,1,6,5,1}	Ours	16ms	103ms	0.052MB
	MD-SONIC	107ms	192ms	0.056MB
CONV _{32,3,6,5,1}	Ours	52ms	154ms	0.071MB
	MD-SONIC	172ms	313ms	0.076MB
CONV _{64,3,64,5,1}	Ours	1080ms	2639ms	3.515MB
	MD-SONIC	2738ms	3293ms	3.736MB
ReLU ₃₂	Ours	4ms	448ms	0.469MB
	Using mult-Trun in MD-SONIC	4ms	653ms	0.203MB
	MD-SONIC	467ms	710ms	0.036MB
	Ours	30ms	1126ms	7.5MB
ReLU ₁₂₈	Using mult-Trun in MD-SONIC	56ms	1205ms	3.25MB
	MD-SONIC	4850ms	5308ms	0.579MB
	Ours	485ms	5867ms	120MB
	Using mult-Trun in MD-SONIC	706ms	6494ms	52MB
ReLU ₅₁₂	MD-SONIC	66.82s	72.49s	9.257MB
Maxpool _{24,16,2}	Ours	35ms	1763ms	3.164MB
	MD-SONIC	2343ms	2727ms	0.244MB
Maxpool _{15,96,3}	Ours	94ms	3903ms	8.789MB
	MD-SONIC	5637ms	6656ms	0.678MB
Maxpool _{56,64,2}	Ours	318ms	4892ms	68.906MB
	MD-SONIC	36.06s	39.59s	5.315MB
BN ₃₂	Ours	0ms	51ms	0.016MB
BN ₁₂₈	Ours	3ms	584ms	0.25MB
BN ₅₁₂	Ours	94ms	1656ms	4MB

- WAN: 100ms network delay, 1% packet loss rate, and 100Mbps bandwidth.
- LAN: 1ms network delay, 0.01% packet loss rate, and 10Gbps bandwidth.

Computational parameters: We set $l = 64$ bits for ring element representation and set $d = 16$ for fractional bits of fixed-point arithmetic.

Time and communication overhead: For time overhead, we define it as the duration from the moment all entities involved in the computation task begin until the last entity completes the task. For communication overhead, it is defined as the amortized value per participating entity.

B. Microbenchmarks of Building Blocks

In this section, we present detailed benchmarking data for the fundamental building blocks of our design. Due to space limitations, we have written the analysis of $\Pi_{mult-exp}$ in the supplementary file.

1) Analysis of multiplication protocol: TABLE V demonstrates the improvements in computational and communication overheads of Π_{mult} compared to $\Pi_{Asterisk-mult}$ under 2-5 participating parties.

2) Analysis of two-party polynomial protocol: Error! Reference source not found. compares the computational and

> REPLACE THIS LINE WITH YOUR MANUSCRIPT ID NUMBER (DOUBLE-CLICK HERE TO EDIT) <

TABLE VIII
PERFORMANCE OF NEURAL NETWORK INFERENCE WITH
OUR FRAMEWORK AND MD-SONIC ON LeNet

Dataset	Framework	LAN	WAN	Comm.
MNIST	ours without BN	78ms	2599ms	1.3MB
	ours with BN	98ms	1939ms	3.39MB
	MD-SONIC	1681ms	3515ms	0.24MB
CIFAR-10	ours without BN	102ms	2733ms	1.3MB
	ours with BN	121ms	2073ms	3.39MB
	MD-SONIC	2287ms	3828ms	0.34MB
Tiny ImageNet	ours without BN	691ms	7470ms	7.08MB
	ours with BN	709ms	6173ms	20.6MB
	MD-SONIC	9834ms	12.59s	1.69MB

communication overheads of implementing two-party fixed-point polynomial evaluation using $\Pi_{two-poly}$ and $\Pi_{mult-Trun}$.

3) Analysis of NN building blocks: We benchmark the online costs of NN building blocks in TABLE VI. **To the best of our knowledge**, we provide the first implementation of complete NN building blocks within the HA-MSDM model.

C. Benchmarks on Secure Inference

In this section, we measured the online time overhead and communication overhead of secure inference using different datasets under the LeNet and AlexNet networks. As we focus on the secure inference phase, the experimental results presented in this section exclude the input and output processes. To mitigate the issue of escaping activation, we incorporate a BN layer prior to the activation function. For fair comparison, we provide data for NN inference both with and without BN layers. In networks with BN layers, we employ $\Pi_{two-poly}$ to implement the ReLU activation, whereas in networks without BN layers, we utilize $\Pi_{mult-Trun}$ for ReLU implementation. This is due to the requirement of $\Pi_{two-poly}$ to constrain the input range for correctness. Note that network layers without BN layers in our framework cannot perform accurate privacy inference. We record these statistics solely to provide fair comparisons under identical network architectures and to demonstrate the superiority of $\Pi_{two-poly}$.

1) Analysis of LeNet: TABLE VIII presents the performance of NN inference using our framework and MD-SONIC under the LeNet network with the MNIST, CIFAR-10, and Tiny-ImageNet datasets in LAN and WAN settings.

2) Analysis of AlexNet: As shown in TABLE VII, we present data on NN inference for our framework and MD-SONIC using the AlexNet network with the CIFAR-10, Tiny-ImageNet, and ImageNet datasets under LAN and WAN settings.

VII. CONCLUSION

In this work, we propose the first private inference framework in HA-MSDM model. Initially, we develop efficient fixed-round MPC protocols. Subsequently, we proposed a private inference strategy combining fixed-interval high-precision polynomial approximation with parameter-adjusted BN layer. Finally, we analyzed our framework through

TABLE VII
PERFORMANCE OF NEURAL NETWORK INFERENCE WITH
OUR FRAMEWORK AND MD-SONIC ON ALEXNET

Dataset	Framework	LAN	WAN	Comm.
CIFAR-10	ours without BN	3203ms	8984ms	3.21MB
	ours with BN	3187ms	8274ms	9.37MB
	MD-SONIC	7576ms	11.14s	1.15MB
Tiny ImageNet	ours without BN	5953ms	18.85s	7.99MB
	ours with BN	5752ms	16.96s	21.68MB
	MD-SONIC	147.7s	161.1s	22.28MB
Image-Net	ours without BN	61.72s	113.2s	195.4MB
	ours with BN	61.92s	108.4s	590.1MB
	MD-SONIC	324.3s	344.4s	33.94MB

microbenchmarks of building blocks and benchmarks of private inference. Our framework incurs higher communication overhead due to polynomial approximation and fixed-round polynomial protocols, but it demonstrates significant advantages in time efficiency due to reduced communication rounds and parallelized processing. We outline several potential future research directions: (1) exploring primitive implementations under higher output security guarantees, and (2) leveraging hardware acceleration, such as GPUs, to enhance efficiency.

REFERENCES

- [1] L. K. L. Ng and S. S. M. Chow, "SoK: Cryptographic neural-network computation," in *Proc. IEEE Symp. Secur. Privacy (SP)*, May 2023, pp. 497–514.
- [2] Y. Li, Y. Wang, Q. Fan, Z. Pan, Y. Wu, Z. Zhang, L. Zhu, and W. Zhou, "Secure Multi-party Learning: Fundamentals, Frameworks, State of the Art, Trends, and Challenges," *IEEE Trans. Netw. Sci. Eng.*, 2025, pp. 1–25.
- [3] A. C. Yao, "Protocols for secure computations," in *Proc. 23rd Annu. Symp. Found. Comput. Sci. (SFCS)*, Nov. 1982, pp. 160–164.
- [4] E. Chen, J. Zhu, A. Ozdemir, R. S. Wahby, F. Brown, and W. Zheng, "Silph: A framework for scalable and accurate generation of hybrid MPC protocols," in *Proc. IEEE Symp. Secur. Privacy (SP)*, May 2023, pp. 848–863.
- [5] J.-L. Watson, S. Wagh, and R. A. Popa, "Piranha: A GPU platform for secure computation," in *Proc. 31st USENIX Secur. Symp. (USENIX Secur.)*, 2022, pp. 827–844.
- [6] F. Liu, X. Xie, and Y. Yu, "Scalable multi-party computation protocols for machine learning in the honest-majority setting," in *Proc. 33rd USENIX Secur. Symp. (USENIX Secur.)*, 2024, pp. 1939–1956.
- [7] N. Koti, M. Pancholi, A. Patra, and A. Suresh, "SWIFT: Super-fast and robust privacy-preserving machine learning," in *Proc. 30th USENIX Secur. Symp. (USENIX Secur.)*, 2021, pp. 2651–2668.
- [8] S. Wagh, S. Tople, F. Benhamouda, E. Kushilevitz, P. Mittal, and T. Rabin, "FALCON: Honest-majority maliciously secure framework for private deep learning," *Proc. Privacy Enhancing Technol.*, vol. 2021, no. 1, pp. 188–208, Jan. 2021.
- [9] B. Yuan, S. Yang, Y. Zhang, N. Ding, D. Gu, and S.-F. Sun, "MD-ML: Super fast privacy-preserving machine learning for malicious security with a dishonest majority," in *Proc. 33rd USENIX Secur. Symp. (USENIX Secur.)*, 2024, pp. 2227–2244.
- [10] Y. Zhang, X. Chen, Y. Dong, Q. Zhang, R. Hou, Q. Liu, and X. Chen, "MD-SONIC: Maliciously-Secure Outsourcing Neural Network Inference With Reduced Online Communication," *IEEE Trans. Inf. Forensics Security*, vol. 20, pp. 3534–3549, 2025.
- [11] C. Richard, "Limits on the security of coin flips when half the processors are faulty," in *ACM STOC*, 1986, pp. 264–369.
- [12] B. Karmakar, N. Koti, A. Patra, S. Patranabis, P. Paul, and D. Ravi,

> REPLACE THIS LINE WITH YOUR MANUSCRIPT ID NUMBER (DOUBLE-CLICK HERE TO EDIT) <

- “Asterisk: Super-fast MPC with a Friend,” in *Proc. IEEE Symp. Secur. Privacy (SP)*, 2024, pp. 542–560.
- [13] Q. Pang, J. Zhu, H. Möllering, W. Zheng and T. Schneider, 2024, May. “Bolt: Privacy-preserving, accurate and efficient inference for transformers,” in *Proc. IEEE Symp. Secur. Privacy (SP)*, 2024, pp. 4753–4771.
- [14] S. U. Hussain, M. Javaheripi, M. Samragh, and F. Koushanfar, “COINN: Crypto/ML codesign for oblivious inference via neural networks,” in *Proc. ACM SIGSAC Conf. Comput. Commun. Secur.*, 2021, pp. 3266–3281.
- [15] Z. Ghodsi, A. K. Veldanda, B. Reagen, and S. Garg, “CryptoNAS: Private inference on a ReLU budget,” in *Proc. Adv. Neural Inf. Process. Syst.*, 2020, vol. 33, pp. 16961–16971.
- [16] K. Garimella, N. K. Jha, and B. Reagen, “Sisyphus: A cautionary tale of using low-degree polynomial activations in privacy-preserving deep learning,” in *Proc. Privacy Preserving Mach. Learn. Workshop (PPML@ACM CCS)*, 2021, pp. 1–6.
- [17] A. Diaa et al., “Fast and Private Inference of Deep Neural Networks by Co-designing Activation Functions,” in *Proc. 33rd USENIX Secur. Symp. (USENIX Secur.)*, 2024, pp. 2191–2208.
- [18] R. Gilad-Bachrach, N. Dowlin, K. Laine, K. Lauter, M. Naehrig, and J. Wernsing, “CryptoNets: Applying neural networks to encrypted data with high throughput and accuracy,” in *Proc. Int. Conf. Mach. Learn.*, 2016, pp. 201–210.
- [19] H. Chabanne, A. de Wargny, J. Milgram, C. Morel, and E. Prouff, “Privacy-preserving classification on deep neural network,” *IACR Cryptol.*, vol. 2017, no. 35, pp. 1–18, 2017.
- [20] E. Hesamifard, H. Takabi, M. Ghasemi, and E. Witchel, “Privacy-preserving machine learning as a service,” in *Proc. Privacy Enhancing Technol.*, vol. 2018, no. 3, pp. 123–142, 2018.
- [21] W. Z. Srinivasan, PMRL Akshayaram, and P. R. Ada, “Delphi: A cryptographic inference service for neural networks,” in *Proc. 29th USENIX Secur. Symp.*, 2019, pp. 2505–2522.
- [22] P. Mohassel and Y. Zhang, “SecureML: A system for scalable privacy-preserving machine learning,” in *Proc. IEEE Symp. Secur. Privacy (SP)*, 2017, pp. 19–38.
- [23] I. Damgård, M. Keller, E. Larraia, V. Pastro, P. Scholl, and N. P. Smart, “Practical covertly secure MPC for dishonest majority—or: Breaking the SPDZ limits,” in *Proc. 18th Eur. Symp. Res. Comput. Secur.*, Egham, U.K. Cham, Switzerland: Springer, 2013, pp. 1–18.
- [24] I. Damgård, V. Pastro, N. P. Smart, and S. Zakarias, “Multiparty computation from somewhat homomorphic encryption,” in *Proc. Annu. Int. Cryptol. Conf. (CRYPTO)*. Cham, Switzerland: Springer, 2012, pp. 643–662.
- [25] M. Keller, E. Orsini, and P. Scholl, “MASCOT: Faster malicious arithmetic secure computation with oblivious transfer,” in *Proc. ACM SIGSAC Conf. Comput. Commun. Secur.*, Oct. 2016, pp. 830–842.
- [26] M. Keller, V. Pastro, and D. Rotaru, “Overdrive: Making SPDZ great again,” in *Proc. Int. Conf. Theory Appl. Cryptograph. Techn. (EUROCRYPT)*. Cham, Switzerland: Springer, 2018, pp. 158–189.
- [27] R. Cramer, I. Damgård, D. Escudero, P. Scholl, and C. Xing, “SPDZ_{2k}: Efficient MPC mod 2^k for dishonest majority,” in *Proc. Annu. Int. Cryptol. Conf.* Cham, Switzerland: Springer, 2018, pp. 769–798.
- [28] E. Orsini, N. P. Smart, and F. Vercauteren, “Overdrive2k: Efficient secure MPC over from somewhat homomorphic encryption,” in *Proc. Cryptographer Track RSA Conf.*, 2020, pp. 254–283.
- [29] N. Chandran, W. Chongchitmate, R. Ostrovsky, and I. Visconti, “Universally Composable Secure Computation with Corrupted Tokens,” In *CRYPTO*, pp 432–461, 2019.
- [30] H. Carmit, P. Antigoni, and V. Muthuramakrishnan, “Composable security in the tamper-proof hardware model under minimal complexity,” In *TCC*, pp 367–399, 2016.
- [31] B. Saikrishna, J. Abhishek, O. Rafail, and V. Ivan, “Non-interactive secure computation from one-way functions,” In *ASIACRYPT*, pp 118–138, 2018.
- [32] Y. Ishai, A. Patra, S. Patranabis, D. Ravi, and A. Srinivasan, “Fully-Secure MPC with Minimal Trust,” in *TCC*, vol. 13748, pp. 470–501, 2022.
- [33] P. Muth and S. Katzenbeisser, “Assisted Multi-Party Computation,” *Cryptology ePrint Archive*, 2022.
- [34] J. Lee, E. Lee, J.-W. Lee, Y. Kim, Y.-S. Kim, and J.-S. No, “Precise approximation of convolutional neural networks for homomorphically encrypted data,” *arXiv:2105.10879*, 2021.
- [35] B. Alon, E. Omri, and A. Paskin-Cherniavsky, “MPC with friends and foes,” In *CRYPTO*, pp. 677–706, 2020.
- [36] D. Lu, T. Yurek, S. Kulshreshtha, R. Govind, A. Kate, and A. Miller, “HoneyBadgerMPC and AsynchroMix: Practical asynchronous MPC and its application to anonymous communication,” in *Proc. ACM SIGSAC Conf. Comput. Commun. Secur.*, Nov. 2019, pp. 887–903.